

Hydromagnetic non-newtonian fluid flow between parallel semi infinite vertical plates

Research Article

Osiemo Michael Ong'ong'a^a, *, Mathew Kinyanjui^b, Kang'ethe Giterere^c

^a Department of Mathematics, Pan African University, Institute for Basic Science, Technology and Innovation, Juja, 62000-00200, Nairobi, Kenya

^b Department of Pure and Applied Mathematics, Jomo Kenyatta University, Juja, 62000-00200, Nairobi, Kenya

^c Department of Pure and Applied Mathematics, Jomo Kenyatta University, Juja, 62000-00200, Nairobi, Kenya

Received 05 February 2022; accepted (in revised version) 09 March 2022

Abstract: The incompressible, laminar, electrically conducting, non-Newtonian fluid flow past two porous vertical semi-infinite plates is investigated in the presence of inclined variable magnetic field. The governing equations of momentum, energy equation and induction equation have been solved numerically using the trivariate spectral relaxation collocation method, and implemented using computer software. The results have been presented graphically. The velocity, temperature and induction profiles and the effect of variable inclined magnetic field and variable viscosity on flow variables have been determined. The effects of Reynolds number, Prandtl number, Magnetic parameter, thermal Grashof number, magnetic Reynolds number, Eckert number and injection parameter on flow variables velocity, temperature and magnetic induction profiles has been investigated. When the parameters are changed, the velocity, temperature, and induction profiles are observed to increase, decrease, or have no effect. This research has a broad array of applications in industry, science, and technology, including geothermal reservoirs, MHD generators, the agricultural sector, cooling system design, plasma investigations, and many more.

MSC: 76A05 • 85A30

Keywords: Non-Newtonian fluid • Semi-infinite plates • Variable magnetic field

© 2022 The Author(s). This is an open access article under the CC BY-NC-ND license (<https://creativecommons.org/licenses/by-nc-nd/3.0/>).

1. Introduction

The term "hydrodynamics" is derived from two words: "hydro," which means "water," and "dynamics," which means "motion under the influence of force". Hydrodynamics is the science that is concerned with the flow of liquids. Magneto-hydrodynamics is a science that combines fluid dynamics and electromagnetism to analyze the movement of an electrically conducting fluid. Examples of electrically conducting fluids include plasma, molten metals, and electrolytes. A magnetic field can produce a retarding or accelerating force as well as an inducing electric field and current in the flow of an electrically conducting fluid. The induced electric current also generates an induced magnetic field, which modifies the initial attractive field. The fluid particles are constrained by the two-way interaction of the flow field and magnetic field. Hydro-magnetic flows are more complex than conventional hydrodynamic flows. Momentum, energy and magnetic induction equations are the governing equations to be solved.

* Corresponding author.

E-mail address(es): michaelosiemog@gmail.com (Osiemo Michael Ong'ong'a), mathewkiny@jkuat.ac.ke (Mathew Kinyanjui), kngit@itc.jkuat.ac.ke (Kang'ethe Giterere).

Fluids are classified as Newtonian or Non-Newtonian depending on their properties. Non-Newtonian fluids do not follow Newton's law of viscosity, hence their viscosity varies. According to [1] the viscosity and shear stress of these fluids are proportional. [2] investigated the unsteady fluid flow between two moving parallel porous plates in the presence of an inclined applied magnetic field. In this study, horizontal parallel plates moving at a uniform velocity at $t > 0$ in existence of inclined uniform applied magnetic field was considered. The flow model were solved by method of Crank-Nickson and simulated using MATLAB software. It concluded that the velocity profile of the fluid flow increased with an increase in the magnetic parameter M , Reynold's number Re , the magnetic inclination and the injection parameter S_0 .

[3] investigated the Magnetohydrodynamic flow between two parallel plates in the presence of an inclined magnetic field. To solve the governing equations, he employed the finite difference method (FDM). The study looked at horizontal plates with the upper plate moving at a constant speed and the lower plate remaining fixed. A stable, Newtonian, laminar, and incompressible fluid is subjected to a constant pressure gradient. [4] pursued Non-Newtonian fluid flow and heat transfer characteristics across an oscillating flat plate. Non-Newtonian incompressible fluid flows continuously in two dimensions through a porous media constrained by an infinite vertical porous plate subjected to uniform suction under the influence of a uniform transverse magnetic field, according to [5]. The perturbation technique was used to approximate flow variables. [6] studied the effects of heat and mass transfer on the motion of non-Newtonian nanofluid over an infinite permeable flat plate. [7] investigated unsteady MHD couette fluid flow between two parallel porous medium plates in an inclined magnetic field. [8] studied the impacts of porosity on the flow of mhd Flow convection. In a rotating system, a moving vertical plate with ramped temperature and radiation is ramped. Unsteady MHD couette flow through porous plates of a viscous, incompressible fluid flow between two horizontal parallel porous plates under the influence of thermal radiation and chemical reaction was considered by [9]. In a rotating system, [10] studied turbulent hydromagnetic flow with thermal radiation heat over a moving embedded in a porous medium. A uniform transverse magnetic field is applied to the plates in a normal direction. [11] studied the unsteady two-dimensional Jeffery-Hamel laminar flow of an incompressible non-Newtonian fluid with non-linear viscosity flowing through a divergent wedge-shaped in the presence of a uniform applied magnetic field in the direction normal to the fluid flow.

[1] analyzed hydro-magnetic flow of a non-Newtonian fluid in a porous medium induced by a moving plate in the presence of inclined magnetic field. Researcher adopted finite difference numerical method to solve governing equations. Researcher calculated the temperature and velocity profiles of a fluid flow. Researcher studied the effects of the various parameters on flow variables. The uniform magnetic field was applied to a non-Newtonian, incompressible, unsteady fluid flowing through two parallel horizontal plates with upper plate moving at a constant velocity was considered. [12] investigated hydro-magnetic couette flow between two vertical semi-infinite porous plates with uniform injection/suction in the presence of an uniform magnetic field, applying normal to the fluid flow and taking joule heating into account. The flow models were solved using the FDM, and the results were analysed and graphically represented using MATLAB software. The researchers investigated the effects of parameters on the velocity and temperature profiles of a fluid flow.

2. Mathematical Formulation

The fluid is assumed to be incompressible, non-Newtonian and laminar flowing past two vertical, stationary and parallel semi-infinite plates placed at $X=0$ and $X=H$ in z and y direction, in the presence of inclined magnetic field. The variable magnetic field is applied at an angle α to (y,z) plane. when $t = 0$, the fluid is assumed to be flowing with free stream velocity U_∞ , magnetic field \vec{B} and $T = T_\infty$. The plates are assumed to be non-conducting and uniformly porous, no applied external electric field, no chemical reactions and Electrical conductivity is a constant.

3. Governing equations

In this research, the flow governing equations are the momentum equation, energy equation, and induction equation.

3.1. Equation of the motion

$$\rho_\infty \left(\frac{\partial \vec{V}}{\partial t} + (\vec{V} \cdot \nabla) \vec{V} \right) = -\nabla p + \mu \nabla^2 \vec{V} + \rho \vec{F}_B \quad (1)$$

Where F are the body forces Lorentz force F_l and gravitational force F_g . $\vec{V} = (u, v, 0)$ is the velocity vector, $\vec{B} = (b_x + B \cos \alpha, b_y + B \sin \alpha, 0)$ is the magnetic field vector with $(b_x, b_y, 0)$ is the induced magnetic field along x and y direction.

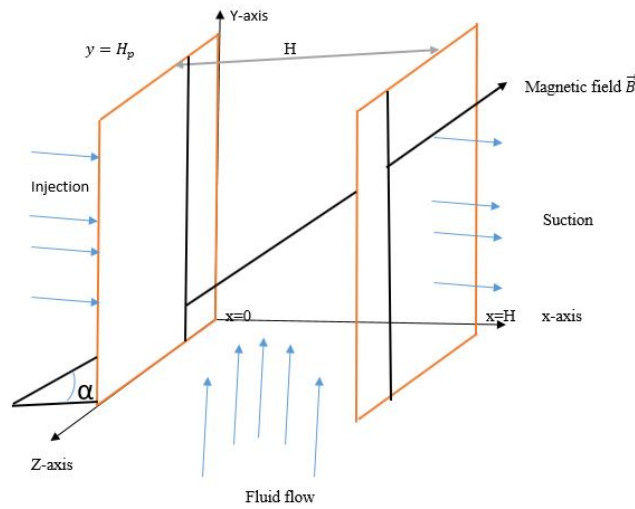


Fig. 1. Geometry configuration

μ is a dynamic viscosity assumed to have linear relationship with temperature by [13]

$$\mu(T) = \frac{\mu_\infty}{1 + \gamma(T - T_\infty)} \tag{2}$$

Where $\vec{J} = (j_x, j_y, 0)$ and

$$\vec{J} = \sigma (\vec{V} \times \vec{B}) \tag{3}$$

$$\vec{J} = \sigma (u(b_y + B \sin \alpha) - v B_x) \hat{k} \tag{4}$$

Lorentz force $F_l = \vec{J} \times \vec{B}$

$$F_l = \sigma (v(b_x + B \cos \alpha)(b_y + B \sin \alpha) - u(b_y + B \sin \alpha)^2) \hat{i} \tag{5}$$

$$+ \sigma (u(b_x + B \cos \alpha)(b_y + B \sin \alpha) - v(b_x + B \cos \alpha)^2) \hat{j} \tag{6}$$

The body forces considered in this study are Lorentz force, gravitational force and viscous force. The velocity along x direction is constant and therefore, momentum equation (1) reduce to

$$0 = \frac{\sigma}{\rho_\infty} (v(b_x + B \cos \alpha)(b_y + B \sin \alpha) - u(b_y + B \sin \alpha)^2) - \frac{1}{\rho_\infty} \left(\frac{\mu_\infty}{[1 + \gamma(T - T_\infty)]} \right) \frac{u}{k_p} \tag{7}$$

$$\frac{\partial v}{\partial t} + u \frac{\partial v}{\partial x} = \frac{1}{\rho_\infty} \left(\frac{\mu_\infty}{[1 + \gamma(T - T_\infty)]} \right) \left(\frac{\partial^2 v}{\partial x^2} \right) + \frac{\sigma}{\rho_\infty} (u(b_x + B \cos \alpha)(b_y + B \sin \alpha) - v(b_x + B \cos \alpha)^2) + \beta g (T - T_\infty) \tag{8}$$

3.2. Energy equation

$$\rho_\infty C_p \left(\frac{\partial T}{\partial t} + u \frac{\partial T}{\partial x} + v \frac{\partial T}{\partial y} \right) = k \left(\frac{\partial^2 T}{\partial x^2} + \frac{\partial^2 T}{\partial y^2} \right) + \mu \phi + \frac{j^2}{\sigma} \tag{9}$$

The viscous dissipation function ϕ in two dimensions

$$\phi = 2 \left[\left(\frac{\partial u}{\partial x} \right)^2 + \left(\frac{\partial v}{\partial y} \right)^2 \right] + \left(\frac{\partial u}{\partial y} + \frac{\partial v}{\partial x} \right)^2 \tag{10}$$

In this study, viscous dissipation reduces to

$$\phi = \left(\frac{\partial v}{\partial x} \right)^2$$

The fluid's thermal conductivity is assumed to be a linear function of temperature from the paper written [13] .

$$k = k_{\infty} (1 + \eta (T - T_{\infty})) \quad (11)$$

The Joules heating term becomes

$$\frac{j^2}{\sigma} = \sigma (uB_y - vB_x)^2 \quad (12)$$

Substituting these terms to energy equation (9), we obtained

$$\begin{aligned} \rho_{\infty} C_p \left(\frac{\partial T}{\partial t} + v \frac{\partial T}{\partial y} \right) &= k_{\infty} \eta \left(\frac{\partial T}{\partial y} \right)^2 + k_{\infty} (1 + \eta (T - T_{\infty})) \left(\frac{\partial^2 T}{\partial y^2} \right) \\ &+ \left(\frac{\mu_{\infty}}{1 + \gamma (T - T_{\infty})} \right) \left(\frac{\partial v}{\partial x} \right)^2 + \sigma (u(b_y + B \sin \alpha) - v(b_x + B \cos \alpha))^2 \end{aligned} \quad (13)$$

3.3. Induction equation

$$\frac{\partial \vec{B}}{\partial t} = \nabla \times (\vec{V} \times \vec{B}) + \frac{1}{\sigma \mu_e} \nabla^2 \vec{B} \quad (14)$$

where $\frac{1}{\sigma \mu_e}$ is magnetic diffusivity of the fluid.

Substituting the components of induction equations and Collecting the terms in i and j, equation (14) becomes

$$\left\{ \begin{aligned} \frac{\partial b_x}{\partial t} + u \frac{\partial b_x}{\partial x} + v \frac{\partial b_x}{\partial y} &= \frac{1}{\sigma \mu_e} \left(\frac{\partial^2 b_x}{\partial x^2} + \frac{\partial^2 b_x}{\partial y^2} \right) \\ \frac{\partial b_y}{\partial t} + u \frac{\partial b_y}{\partial x} + v \frac{\partial b_y}{\partial y} &= (b_x + B \cos \alpha) \frac{\partial v}{\partial x} + \frac{1}{\sigma \mu_e} \left(\frac{\partial^2 b_y}{\partial x^2} + \frac{\partial^2 b_y}{\partial y^2} \right) \end{aligned} \right. \quad (15)$$

The initial conditions

at $t = 0$

$$v = U_{\infty}, \quad u = 0, \quad T = T_i, \quad b_x = 0, \quad b_y = 0$$

The boundary conditions are; At $t > 0$

$$y = 0 \quad \text{and} \quad 0 \leq x \leq H: \quad v = U_{\infty}, \quad T = T_{\infty}, \quad b_x = B, \quad b_y = B$$

$$y = H_p \quad \text{and} \quad 0 \leq x \leq H: \quad v = U_{\infty}, \quad T = T_{\infty}, \quad b_x = B, \quad b_y = B$$

$$x = 0 \quad \text{and} \quad 0 \leq y \leq H_p: \quad u = u_0, \quad T = T_{\infty}, \quad b_x = B, \quad b_y = B$$

$$x = H \quad \text{and} \quad 0 \leq y \leq H_p: \quad u = -u_0, \quad T = T_{\infty}, \quad b_x = B, \quad b_y = B$$

3.4. Non-Dimensionalization

The following are characteristic quantities are used in non-dimensionalization process.

$$\begin{aligned} v^* &= \frac{v}{U_{\infty}} \quad x^* = \frac{x}{H} \quad y^* = \frac{y}{H_p} \quad b_x^* = \frac{b_x}{B} \quad b_y^* = \frac{b_y}{B} \quad t^* = \frac{U_{\infty} t}{H_p} \quad \theta = \frac{T - T_{\infty}}{T_i - T_{\infty}} = \frac{T - T_{\infty}}{\Delta T} \\ v &= v^* U_{\infty} \quad x = x^* H \quad y = y^* H_p \quad b_x = b_x^* B \quad b_y = b_y^* B \quad t = \frac{t^* H_p}{U_{\infty}} \quad T = \theta \Delta T + T_{\infty} \end{aligned}$$

The non-dimensional governing equations are

Momentum equation

$$\begin{aligned} \frac{\partial v^*}{\partial t^*} + A_h S \frac{\partial v^*}{\partial x^*} &= \frac{A_h^2}{Re} \left(\frac{1}{1 + \gamma \theta \Delta T} \right) \frac{\partial^2 v^*}{\partial x^{*2}} + M \left(S (b_x^* + \cos \alpha) (b_y^* + \sin \alpha) - v^* (b_x^* + \cos \alpha)^2 \right) \\ &+ Gr \theta \end{aligned} \quad (16)$$

Energy equation

$$\begin{aligned} \frac{\partial \theta}{\partial t^*} + v^* \frac{\partial \theta}{\partial y^*} &= \frac{\eta \Delta T}{Re Pr} \left(\frac{\partial \theta}{\partial y^*} \right)^2 + \frac{(1 + \eta \theta \Delta T)}{Re Pr} \frac{\partial^2 \theta}{\partial y^{*2}} + \frac{Ec}{Re} A_h^2 \left(\frac{1}{1 + \gamma \theta \Delta T} \right) \left(\frac{\partial v^*}{\partial x^*} \right)^2 \\ &+ MEc \left(S (b_y^* + \sin \alpha) - v^* (b_x^* + \cos \alpha) \right)^2 \end{aligned} \quad (17)$$

Induction equation

$$\frac{\partial b_x^*}{\partial t^*} + A_h S \frac{\partial b_x^*}{\partial x^*} + v^* \frac{\partial b_x^*}{\partial y^*} = \frac{1}{Rm} \left(A_h^2 \frac{\partial^2 b_x^*}{\partial x^{*2}} + \frac{\partial^2 b_x^*}{\partial y^{*2}} \right) \tag{18}$$

$$\frac{\partial b_y^*}{\partial t^*} + A_h S \frac{\partial b_y^*}{\partial x^*} + v^* \frac{\partial b_y^*}{\partial y^*} = A_h (b_x^* + \cos \alpha) \frac{\partial v^*}{\partial x^*} + \frac{1}{Rm} \left(A_h^2 \frac{\partial^2 b_y^*}{\partial x^{*2}} + \frac{\partial^2 b_y^*}{\partial y^{*2}} \right) \tag{19}$$

The initial conditions in dimensionless form

at $t^* = 0$

$$v^* = 1, \theta = 1, b_x^* = 0, b_y^* = 0$$

The boundary conditions of this study problem are;

At $t^* > 0$

$$y^* = 0 \text{ and } 0 \leq x^* \leq 1: \theta = 0, b_x^* = 1, b_y^* = 1$$

$$y^* = 1 \text{ and } 0 \leq x^* \leq 1: \theta = 0, b_x^* = 1, b_y^* = 1$$

$$x^* = 0 \text{ and } 0 \leq y^* \leq 1: v^* = 0, \theta = 0, b_x^* = 1, b_y^* = 1$$

$$x = 1 \text{ and } 0 \leq y^* \leq 1: v^* = 0, \theta = 0, b_x^* = 1, b_y^* = 1$$

4. Results and Discussion

The trivariate spectral relaxation collocation method was used to obtain the numerical scheme of momentum, energy and induction equation. trivariate spectral relaxation collocation method is used in solving non-linear PDEs in which system of coupled equations are decoupled using Gauss–Seidel approach and relaxation method assumes that all non linear terms are known from the previous iteration. The obtained non-linear PDEs were implemented in MATLAB software and results were displayed graphically.

4.1. Velocity Profiles

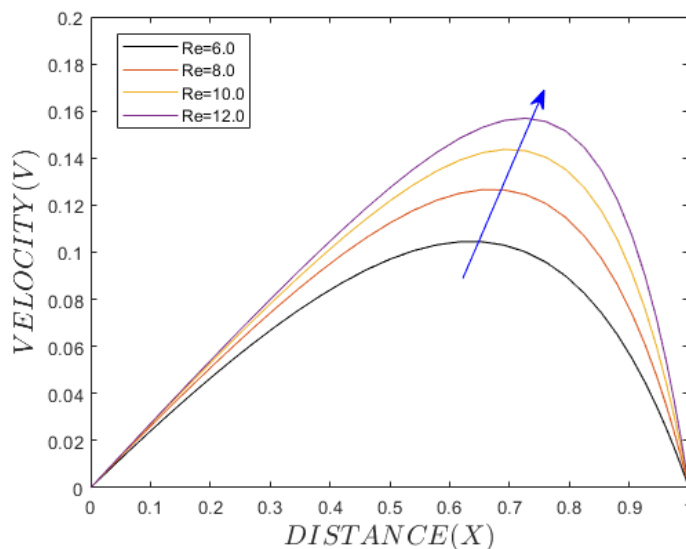


Fig. 2. Effect of Reynolds number on velocity profile fixing M=0.5, Rm = 0.5, Pr = 1.06, Ec = 0.5, $\alpha = 0.52381$, S =3, and Gr = 0.5

From figure 2, Increasing the Reynolds number clearly results in a rise in velocity profiles. The ratio of fluid movement force to viscosity shear force is known as Reynold’s number. Increasing Reynold’s number signifies a decrease in viscous forces that impede fluid motion. As a result, increasing Reynold’s number results in an increase in velocity profile.

From figure 3, It has been observed that, as the magnetic parameter M increases, flow velocity profiles increases as well. The magnetic parameter is the ratio of electromagnetism to viscosity shear force. The magnetic parameter reflects the importance of magnetic induction-induced drag forces in comparison to viscous forces. The magnetic field lines are applied at an angle α in the direction of the fluid flow. The magnetic field line cuts the electrically conducting fluid, hence Lorentz force is generated and the y-component of Lorentz force is positive, hence facilitating the fluid

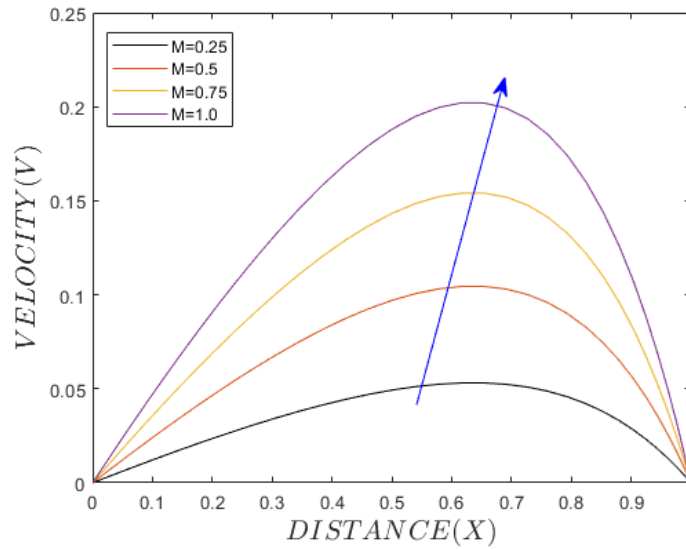


Fig. 3. Effect of magnetic parameter on velocity profile fixing $Re=6.0$, $Rm = 0.5$, $Pr = 1.06$, $Ec = 0.5$, $\alpha = 0.52381$, $S = 3$, and $Gr = 0.5$

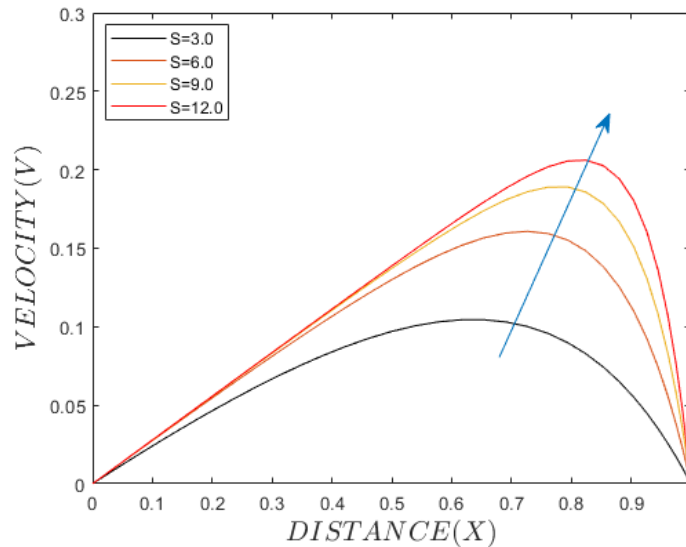


Fig. 4. Effect of injection parameter on velocity profile fixing $Re=6.0$, $Rm = 0.5$, $Pr = 1.06$, $Ec = 0.5$, $\alpha = 0.52381$, $M = 3$, and $Gr = 0.5$

motion. An increase in the magnetic parameter decreases the resistance forces, increasing Lorentz force and therefore increasing fluid velocity profiles.

From Figure 4, The fluid velocity clearly increases as the injection parameter is increased. The injection velocity to free stream velocity ratio is the injection parameter. Injection parameter increases with the increase in injection velocity. The Lorentz force is enhanced by increasing the injection velocity, as calculated from the momentum equation. The Lorentz force is acting in the flow's direction and therefore, the Lorentz force increases as the injection parameter is increased, resulting to an increase in fluid velocity.

From Figure 5, It has been noted that increasing the inclination angle α raises the flow velocity profiles. The inclined magnetic field lines are applied, and the Lorentz force is positive in the y-direction, facilitating the fluid flow. As a result, as the inclination angle increases, the Lorentz force increases, and thus increase in velocity profiles.

4.2. Temperature profile

From Figure 6, it is observed that, increase in Prandtl number leads to increase in temperature profiles. The Prandtl Number is the ratio of momentum to thermal diffusivity. An increase in the Prandtl Number Pr indicates a decrease in the fluid's thermal diffusivity, which leads to an increase in the fluid's internal temperature.

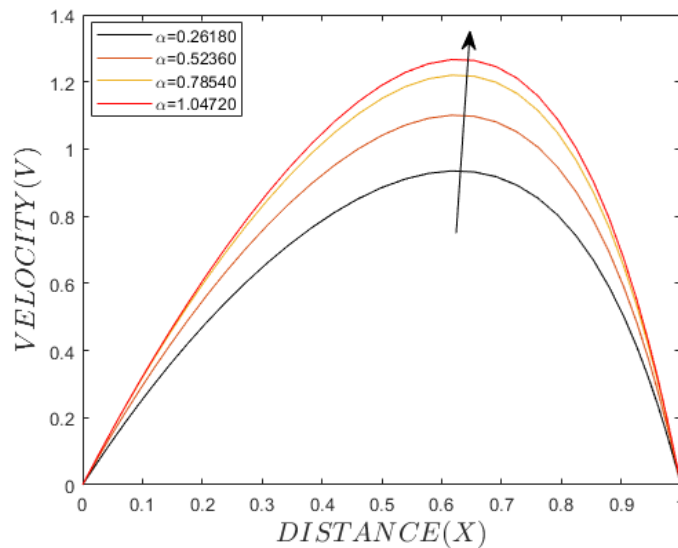


Fig. 5. Effect of angle of inclination on velocity profile fixing $Re=6.0$, $Rm = 0.5$, $Pr = 1.06$, $Ec = 0.5$, $M=3$, $S=3$, and $Gr = 0.5$

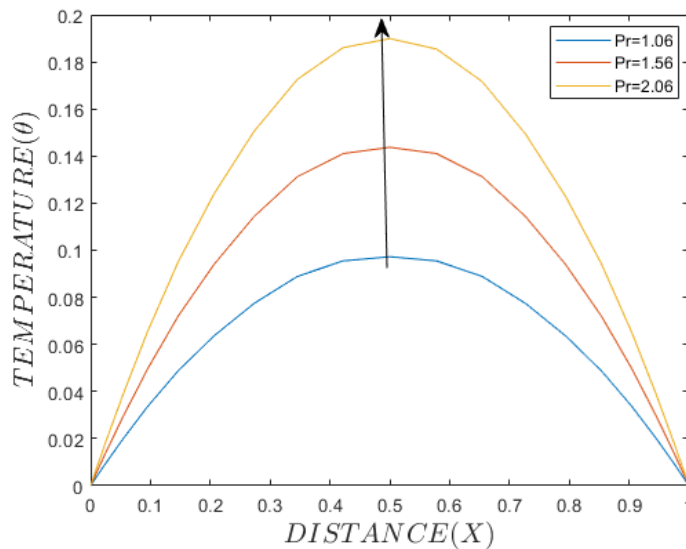


Fig. 6. Effect of Prandtl number on temperature profiles fixing $Re=6.0$, $Rm = 0.5$, $M = 3$, $Ec = 0.5$, $\alpha = 0.52381$, $S=3$, and $Gr = 0.5$

From Figure 7, As the magnetic parameter M increases, the temperature profiles of the fluid rises. The magnetic parameter M is defined as the electromagnetic force divided by the viscosity shear force. Increasing the magnetic parameter M implies decreasing the viscosity shear force and increasing magnetic force by increasing the applied magnetic force. This implies that the fluid velocity increases which leads to increase in collision of fluid particles leading to rise in fluid temperature. Therefore, increase in magnetic parameter leads to increase in temperature profiles.

From Figure 8, it is observed that increasing injection parameter increases the temperature profiles.

Injection parameter is the ratio between the velocity of the fluid between the pores (walls of the porous material) to the free stream velocity. An increase in Injection parameter implies an increase of the injection velocity u_0 . The Joule heating term in Energy equation is increased by increasing the injection velocity. Therefore, increasing S_0 leads to an increase in Joule heating term, and hence, an increase in the temperature profiles.

From Figure 9, The temperature profile of the fluid is found to grow as the Eckert number increases.

The Eckert Number represents the kinetic energy-to-thermal energy ratio. Kinetic energy increases as Ec rises. Increasing Ec leads to increase the kinetic energy. The kinetic energy increases with increasing the fluid velocity. As the fluid velocity increases, the collision of the fluid particles increases causing the dissipation of heat in the boundary layers and hence an increase in fluid temperature.

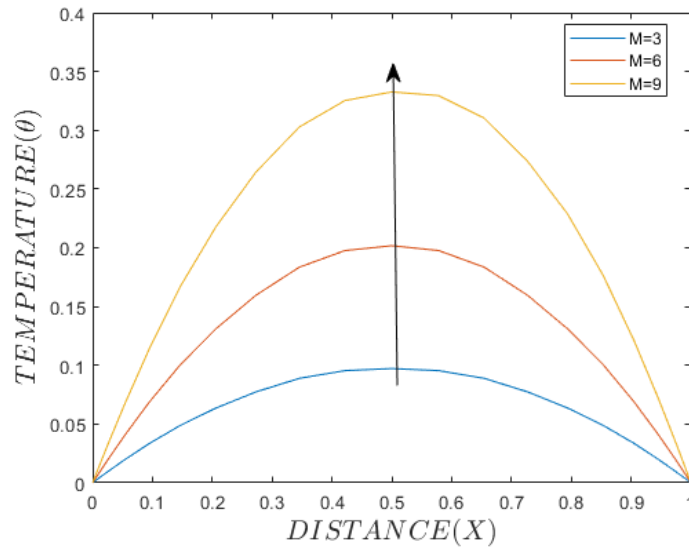


Fig. 7. Effect of magnetic parameter on temperature profile fixing $Re=6.0$, $Rm = 0.5$, $Pr = 1.06$, $Ec = 0.5$, $\alpha = 0.52381$, $S = 3$, and $Gr = 0.5$

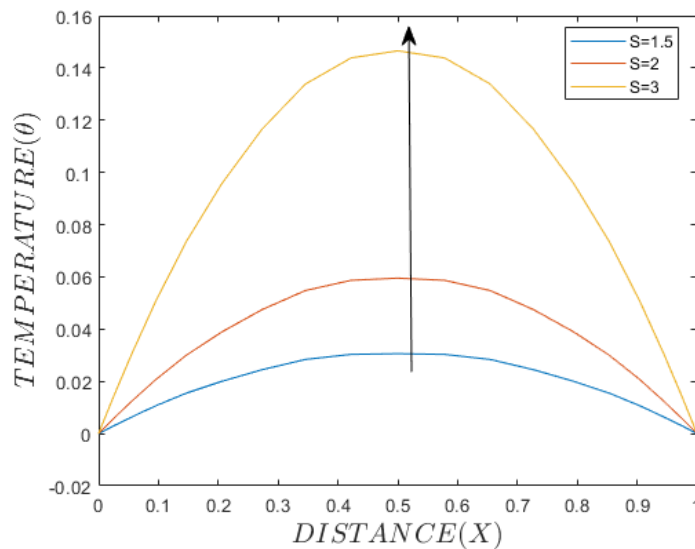


Fig. 8. Effect of injection parameter S on temperature profile fixing $Re=6.0$, $Rm = 0.5$, $Pr = 1.06$, $Ec=0.5$, $\alpha = 0.52381$, $M = 3$, and $Gr = 0.5$

4.3. Induction profile

From Figure 10, the induction profile decreases as the angle of inclination increases.

Increasing the angle of inclination leads to an decrease in magnetic strength which enhances the induced magnetic field. The maximum output is attained when. As the angle of inclination increases, the magnetic field lines tends to become parallel to electrically conducting fluid flow, decreasing the induced magnetic field. Therefore, increasing angle of inclination leads to decrease in induction profile.

From Figure 11, The magnetic induction profiles are observed to increase as the thermal grashof number increases.

Grashof number is dimensionless number in fluid dynamics which approximates the ratio of the buoyancy force to viscous force acting on a fluid. Increasing the Grashof number means decreasing the viscous force, which causes an increase in fluid velocity, which causes an increase in the induced magnetic field. As a result, increasing the Grashof number causes an increase in magnetic induction profiles. From Figure 12, it is noted that, the increase in Reynolds numbers increases the induction profiles.

Reynolds number is the ratio of inertia force to viscous force. Increasing Reynolds number implies reducing viscous force which leads to increase in fluid velocity which leads to increase in Induced magnetic field. Therefore, increase

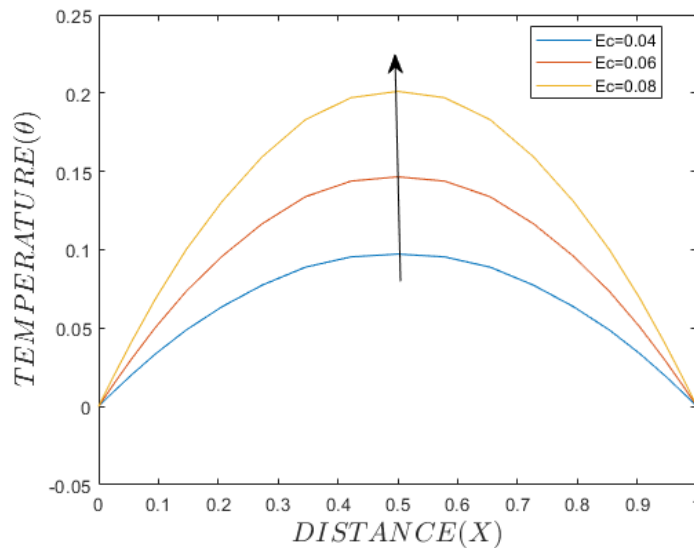


Fig. 9. Effect of Eckert number Ec on temperature profile fixing $Re=6.0$, $Rm = 0.5$, $Pr = 1.06$, $M = 0.5$, $\alpha = 0.52381$, $S=3$, and $Gr = 0.5$

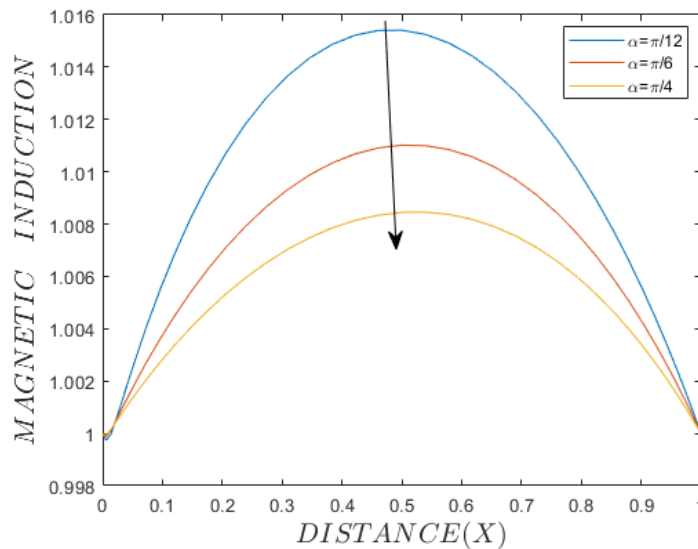


Fig. 10. Effect of angle of inclination on induction profile fixing $Re=6.0$, $Rm = 0.5$, $Pr = 1.06$, $M = 0.5$, $Ec=0.05$, $S=3$, and $Gr = 0.5$

in Reynolds number leads to increase in magnetic induction profiles. From Figure 13, it is noted that, increase suction parameter increases the magnetic induction profiles.

Increasing injection parameters implies increasing injection velocity u_0 which contributes to increase in Lorentz force. The Lorentz force acts in the direction of the flow hence, increasing the velocity of the fluid particle enhancing increase in induced magnetic field. Therefore, increasing injection parameter leads to increase in induction profiles of the flow.

5. Conclusion

In the presence of an inclined variable magnetic field, non-Newtonian fluid flow past two porous vertical semi-infinite plates has been investigated. The resultant model was solved and simulated with MATLAB using the trivariate spectral relaxation collocation method.

The effects of flow parameters have been determined. From the results obtained, the following conclusions have been outlined: The velocity profiles increases with an increase in the magnetic parameter M , Reynold's number Re , the magnetic inclination, and the Injection parameter S .

The temperature profiles increases with the increase in Prandtl number, magnetic parameter, injection parameter

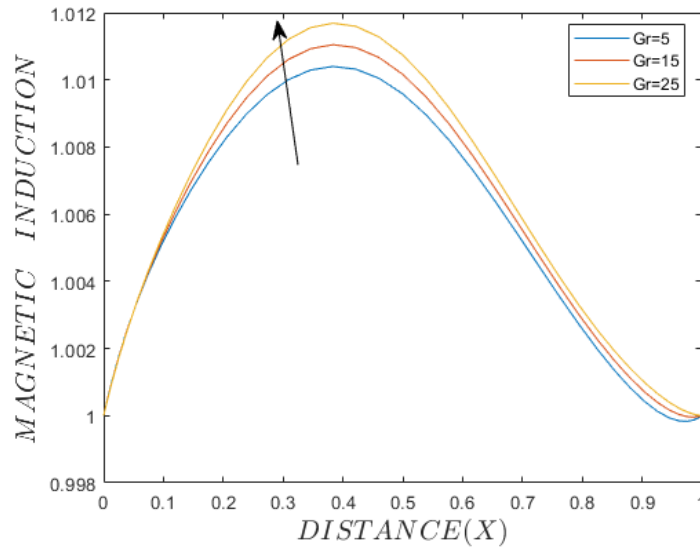


Fig. 11. Effect of Grashof number Gr on induction profile fixing $Re=6.0$, $Rm = 0.5$, $Pr = 1.06$, $M = 0.5$, $\alpha = 0.52381$, $S = 3$, and $Ec = 0.05$

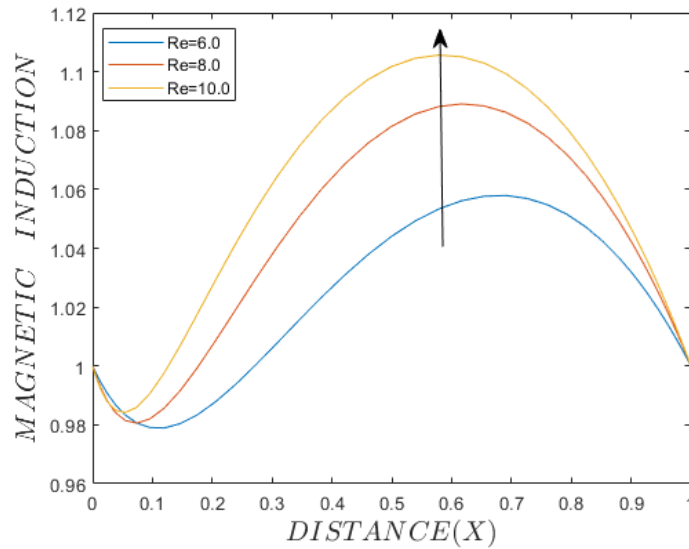


Fig. 12. Effect of Reynolds number Re on induction profile fixing $Ec=0.05$, $Rm = 0.5$, $Pr = 1.06$, $M = 0.5$, $\alpha = 0.52381$, $S = 3$, and $Gr = 0.5$

and Eckert number.

The magnetic induction profile increases with increase in Grashof number, Reynolds number and injection parameter. The induction profile are inversely proportion to the angle of inclination, that is, increase in angle of inclination decreases the magnetic induction profile.

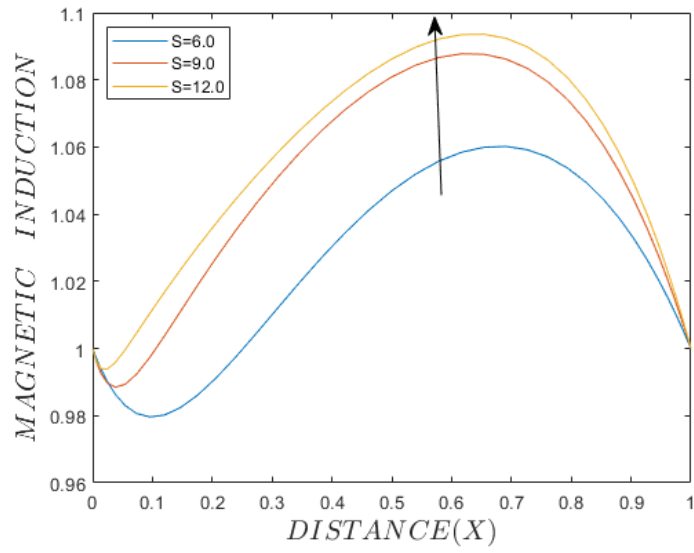


Fig. 13. Effect of injection parameter on induction profile fixing $Re=6.0$, $Rm = 0.5$, $Pr = 1.06$, $M = 0.5$, $\alpha = 0.52381$, $S = 3$, and $Gr = 0.5$

Acknowledgements

The first author wishes to express heartfelt gratitude to the African Union and the Pan African University, Institute for Basic Sciences, Technology, and Innovation for funding and supporting this research.

References

- [1] E. Enock, M. Kinyanjui, et al., *Journal of Applied Mathematics and Bioinformatics* **9**, 15 (2019).
- [2] I. Kane, M. Kinyanjui, and D. Theuri, *Journal of Applied Mathematics and Bioinformatics* **10**, 31 (2020).
- [3] A. D. Aruna Sharma, *International Journal of Innovative Technology and Exploring Engineering (IJITEE)* pp. 4106–4111 (2019).
- [4] A. Chang, K. Vafai, and H. Sun, *Numerical Heat Transfer, Part A: Applications* pp. 1–14 (2021).
- [5] N. H. Ghouri and S. Mustafa, *European Journal of Engineering and Technology* Vol **8** (2020).
- [6] H. M. Shawky, N. T. Eldabe, K. A. Kamel, and E. A. Abd-Aziz, *Heat and mass transfer* **68**, 29 (2020).
- [7] A. Magaji, Tetfund, Tertiary Education Trust Fund (2019).
- [8] U. Rajput and M. Shareef, *Applications & Applied Mathematics* **15** (2020).
- [9] E. Anyanwu, R. Olayiwola, M. Shehu, and A. Lawal, *Asian Research Journal of Mathematics* pp. 1–19 (2020).
- [10] D. N. Ngari, Ph.D. thesis, COPAS, JKUAT (2017).
- [11] F. O. Oochieng, Ph.D. thesis, JKUAT-PAUSTI (2018).
- [12] O. C. Owuora, M. Kinyanjui, and P. Kiogorab (2020).
- [13] S. Mohammad, *Frontiers in Heat and Mass Transfer (FHMT)* **14** (2020).

Submit your manuscript to IJAAMM and benefit from:

- ▶ Rigorous peer review
- ▶ Immediate publication on acceptance
- ▶ Open access: Articles freely available online
- ▶ High visibility within the field
- ▶ Retaining the copyright to your article

Submit your next manuscript at ▶ editor.ijaamm@gmail.com